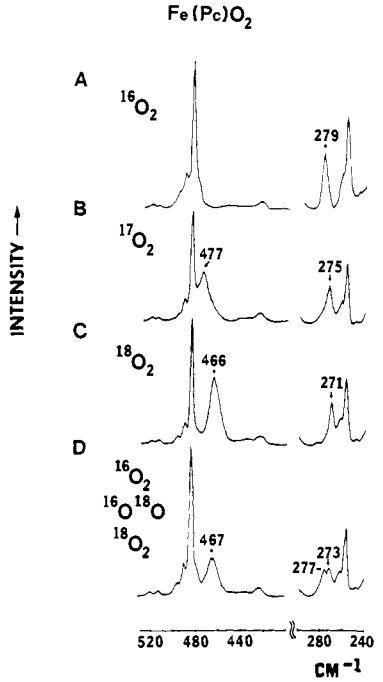

Figure 1. RR spectra of the $Fe(Pc)O_2$ in O_2 matrices at ~15 K (676.4-nm excitation, ~10 mW). The $^{17}O_2$ and $^{18}O_2$ gases used were ~77% and ~98% pure, respectively.

RR spectra as is the case for all other oxyhemoproteins.[1]

Figure 1A shows the RR spectrum of $Fe(Pc)^{16}O_2$ in pure $^{16}O_2$ matrices. The strong band at 486 cm^{-1} and the medium-intensity band at 258 cm^{-1} are due to Fe(Pc) vibrations. However, the band at 279 cm^{-1} is shifted to 275 cm^{-1} by $^{16}O_2$–$^{17}O_2$ substitution (Figure 1B). In addition, this substitution produced a new band at 477 cm^{-1}. Further experiments with $^{18}O_2$ (Figure 1C) shifted these bands to 271 and 466 cm^{-1}, respectively. These results clearly indicate that, in $Fe(Pc)^{16}O_2$, the band corresponding to those at 477 cm^{-1} of $Fe(Pc)^{17}O_2$ and at 466 cm^{-1} of $Fe(Pc)^{18}O_2$ is hidden under the strong Fe(Pc) band at 486 cm^{-1}. Figure 1D shows the RR spectrum of Fe(Pc) cocondensed with a mixture of $^{16}O_2$, $^{16}O^{18}O$, and $^{18}O_2$ in the 1:2:1 ratio. In this case, two bands are observed at around 277 and 273 cm^{-1}.

In order to assign the oxygen isotope sensitive bands, we have carried out normal coordinate calculations on a triatomic Fe–O_I–O_{II} system. According to Jameson et al.,[11] the Fe–O_I (R_1) and O_I–O_{II} (R_2) distances and Fe–O_I–O_{II} angle (α) of $Fe(O_2)(T_{piv}PP)$(2-MeIm)EtOH are 1.90 Å, 1.22 Å, and 129°, respectively. Since no X-ray data are available on $Fe(Pc)O_2$, we varied the molecular dimensions through the following values: R_1 = 1.90–2.00 Å, R_2 = 1.22–1.25 Å, and α = 129–137.5°. Table I shows the results obtained for R_1 = 2.00 Å, R_2 = 1.25 Å, and α = 137.5°. The set of force constants used was $K(R_1)$ = 1.90, $K(R_2)$ = 6.58, and $H(\alpha)$ = 0.22 (all in units of mdyn/Å). Slight changes in force constants gave similar good fits when the molecular dimensions were varied in the above ranges. Most importantly, the potential energy distribution calculations show that for the above set of parameters, the band near 490 cm^{-1} is 70% ν(Fe–O_2) and 27% δ(FeOO), while the band near 280 cm^{-1} is 72% δ(FeOO) and 25% ν(Fe–O_2). However, the degree of mixing decreases as α increases. At the reported angle of 156° for HbO_2,[12] the ~490- and ~280-cm^{-1} bands become ~90% pure ν(Fe–O_2) and δ(FeOO), respectively. Only the use of unreasonably small $K(R_1)$ values (~1.1 mdyn/Å) can reverse these assignments (cf. $K(R_1)$ = 3.08 mdyn/Å of HbO_2[6]).

As shown in Table I, normal coordinate calculations predict the frequency order of the ν(Fe–O_2) rather than the δ(FeOO)[8]

Table I. Comparison of Observed and Calculated Frequencies (cm^{-1})

		$\nu(O_2)$	ν(Fe–O_2)	δ(FeOO)
$(Pc)Fe^{16}O^{16}O$	obsd	1207	488[a]	279
	calcd	1209	490	281
$(Pc)Fe^{16}O^{18}O$	obsd	1176	487[a,b]	273[b]
	calcd	1178	486	273
$(Pc)Fe^{18}O^{16}O$	obsd	1176	467[c]	277[e]
	calcd	1172	470	277
$(Pc)Fe^{18}O^{18}O$	obsd	1144	466	271
	calcd	1140	467	269
$(Pc)Fe^{17}O^{17}O$	obsd		477	275
	calcd	1173	478	275

[a] Expected value. [b] Overlap with $\nu(Fe-^{16}O_2)$. [c] Overlap with $\nu(Fe-^{18}O_2)$. [d] Overlap with $\delta(Fe^{18}O^{18}O)$. [e] Overlap with $\delta(Fe^{16}O^{16}O)$.

to be $Fe^{16}O^{16}O > Fe^{18}O^{16}O < Fe^{16}O^{18}O > Fe^{18}O^{18}O$. In fact, the δ(FeOO) should exhibit a gradual decrease in the above order of isotopic substitution. These trends are entirely opposite to those found for the Fe–CO system.[13] The difference arises because the Fe–CO bond is linear and the central atom (C) is lighter than the terminal atom (O).

The ν(Fe–NO) and δ(FeNO) of Fe^{III}MbNO are at 595 and 573 cm^{-1}, respectively, in solution.[8] These frequencies are close to that of Fe(Pc)NO (580 and 567 cm^{-1}) in a NO matrix at ~15 K.[14] The $\nu(O_2)$ of HbO_2 is ~1130 cm^{-1} in solution,[5] whereas that of $Fe(Pc)O_2$ in an O_2 matrix is 1207 cm^{-1}.[10] In general, the higher the $\nu(O_2)$, the lower the ν(metal–O_2).[15] Hence, the lowering of the ν(Fe–O_2) in going from HbO_2 (567 cm^{-1}) to $Fe(Pc)O_2$ (488 cm^{-1}) is anticipated. These results suggest that the nature of metal–oxygen bonding in the above two compounds does not differ markedly in spite of appreciable differences in their environments.

Acknowledgment. This work was supported by the National Science Foundation, Grant PCM-8114676.

(10) Watanabe, T.; Ama, T.; Nakamoto, K. *J. Phys. Chem.* **1984**, *88*, 440.
(11) Jameson, G. B.; Molinaro, F. S.; Ibers, J. A.; Collman, J. P.; Brauman, J. I.; Rose, E.; Suslick, K. S. *J. Am. Chem. Soc.* **1980**, *102*, 3224.
(12) Shaanan, B. *Nature (London)* **1982**, *296*, 683.
(13) Tsubaki, M.; Srivastava, R. B.; Yu, N.-T. *Biochemistry* **1982**, *21*, 1132.
(14) Bajdor, K.; Proniewicz, L.; Nakamoto, K., manuscript in preparation.
(15) Nakamoto, K.; Nonaka, Y.; Ishiguro, T.; Urban, M. W.; Suzuki, M.; Kozuka, M.; Nishida, Y.; Kida, S. *J. Am. Chem. Soc.* **1982**, *104*, 3386.

Trisubstituted Heteropolytungstates as Soluble Metal Oxide Analogues. 1. The Preparation, Characterization, and Reactions of Organic Solvent Soluble Forms of $Si_2W_{18}Nb_6O_{77}^{8-}$, $SiW_9Nb_3O_{40}^{7-}$, and the $SiW_9Nb_3O_{40}^{7-}$ Supported Organometallic Complex $[(C_5Me_5)Rh{\cdot}SiW_9Nb_3O_{40}]^{5-}$

Richard G. Finke* and Michael W. Droege

Department of Chemistry, University of Oregon
Eugene, Oregon 97403

Received June 1, 1984

Development of polyoxoanions[1a] as discrete, soluble metal oxide analogues[2] has been hampered by the limited number of polyoxoanions containing sufficient charge density at their surface oxygens[1b] to covalently bind transition-metal catalysts. Furthermore, almost nothing is known about how multiple V-, Nb-,

(1) (a) Pope, M. T. In "Heteropoly and Isopoly Oxometalates"; Springer-Verlag: New York: 1983. (b) Classical heteropolyanions such as $PMo_{12}O_{40}^{3-}$ or $SiMo_{12}O_{40}^{4-}$ have been shown to have *less* surface charge density than ClO_4^-: Barcza, L.; Pope, M. T. *J. Phys. Chem.* **1973**, *77*, 1795.
(2) A different approach using metal *alkoxides* as models of metal oxides has appeared:[2a,b] (a) Chisholm, M. H. In "Inorganic Chemistry: Towards the 21st Century"; Chisholm, M. H., Ed.; American Chemical Society: Washington, DC, 1983; ACS Symp. Ser. No. 211, p 243. (b) Chisholm, M. H.; Huffman, J. C.; Leonelli, J.; Rothwell, I. P. *J. Am. Chem. Soc.* **1982**, *104*, 7030 and earlier papers in this series.

0002-7863/84/1506-7274$01.50/0

or other metal-substituted polyoxoanions compare to their parent oxides such as V_2O_5, Nb_2O_5, or M_xO_y.

In 1979 we initiated studies[3] aimed at preparing a series of C_{3v} symmetry, Bu_4N^+ counterion and thus organic solvent soluble, trisubstituted heteropolyanions[4] $SiW_9M_3O_{40}^{x-}$ and $P_2W_{15}M_3O_{62}^{y-}$ (M = V^{5+}, Nb^{5+}, Ta^{5+}, Ti^{4+}, Zr^{4+}, and Hf^{4+}) that we could compare to their parent oxides and which were expected, on the basis of previous work by Stucky,[5] Klemperer, Besecker, Day, and co-workers,[6] and Knoth and Domaille,[7] to possess considerable surface charge density at oxygen for the support of organo-transition-metal catalysts or catalyst precursors.

Herein we report the previously unknown niobium member of the series, $SiW_9Nb_3O_{40}^{7-}$, its dimerization under H^+ to the new type of heteropolyanion $Si_2W_{18}Nb_6O_{77}^{8-}$, $2SiW_9Nb_3O_{40}^{7-} + 6H^+ \rightarrow 3H_2O + Si_2W_{18}Nb_6O_{77}^{8-}$, the interesting parallel of the cleavage reactions of the dimer $Si_2W_{18}Nb_6O_{77}^{8-}$ with H_2O_2, ethanolamine, and OH^- to those of polymeric hydrous niobium oxide,[8] $[Nb_2O_5 \cdot XH_2O]_y$, and the use of the OH^- cleavage product $SiW_9Nb_3O_{40}^{7-}$ to prepare the supported organometallic complex $[(C_5Me_5)Rh \cdot SiW_9Nb_3O_{40}]^{5-}$.

The synthesis of the triniobium heteropolytungstate in its dimeric form from $K_7HNb_6O_{19} \cdot 13H_2O$,[5a,9] A-$\beta$-$Na_9HSiW_9O_{34} \cdot 23H_2O$[10] and acid requires the use of H_2O_2 to solubilize the Nb^{5+} and to prevent Nb_2O_5 formation[11] under the acidic reaction conditions, $K_7HNb_6O_{19} \cdot 13H_2O + 2A\text{-}\beta\text{-}Na_9HSiW_9O_{34} \cdot 23H_2O + 17HCl \rightarrow Si_2W_{18}Nb_6O_{77}^{8-} + 69H_2O + 7K^+ + 18Na^+ + 17Cl^-$. Workup consists of slow $NaHSO_3$ addition to destroy the peroxide, precipitation of the product in 97% yield with $Bu_4N^+Br^-$, and reprecipitation from CH_3CN by aqueous HCl, followed by recrystallization from CH_3CN to provide $(Bu_4N)_6H_2Si_2W_{18}Nb_6O_{77}$ (vide infra) in 70% yield (81 g). Recrystallization from CH_3CN without reprecipitation by aqueous HCl provided $(Bu_4N)_7HSi_2W_{18}Nb_6O_{77}$ in a lower, ca. 50%, yield. Detailed experimental procedures are provided as supplementary material.

Although the anticipated product was $(Bu_4N)_{7-x}H_xSiW_9Nb_3O_{40}$ analogous to the known[4] $K_5H_2SiW_9V_3O_{40}$, the presence of a strong, unusual IR band at 690 cm^{-1} and qualitative differences compared to the chemistry of $(Bu_4N)_4H_3SiW_9V_3O_{40}$[3d] led us to search for alternative formulations. The dimeric, previously unknown $Si_2W_{18}Nb_6O_{77}^{8-}$ formulation and structure (Figure 1A) are supported by solution molecular weight measurements in CH_3CN using the ultracentrifugation sedimentation equilibrium method (calcd for $SiW_9Nb_3O_{40}^{7-}$, 2601; calcd for $Si_2W_{18}Nb_6O_{77}^{8-}$, 5155; calcd for $(Bu_4N)Si_2W_{18}Nb_6O_{77}^{7-}$, 5397; found 5551 (available as supplementary material)), by literature precedent for the 690-cm^{-1} band as a near-linear Nb–O–Nb linkage,[12] by ^{183}W NMR data, and by the elemental analysis. (Anal. for the $6Bu_4N^+$ salt. Anal. Calcd for $C_{96}H_{218}N_6Si_2W_{18}Nb_6O_{77}$: C, 17.44; H, 3.32; N, 1.27; Si, 0.85; W, 50.05; Nb, 8.43. Found: C, 17.40; H, 3.41; N, 1.33; Si, 0.85; W, 50.50; Nb, 8.15. Anal. for the $7Bu_4N^+$ salt. Anal. Calcd for $C_{112}H_{253}N_7Si_2W_{18}Nb_6O_{77}$: C, 19.63; H, 3.71; N, 1.43. Found: C, 19.66; H, 3.74; N, 1.44.) A fast atom bombardment mass spectrum (FABMS) of $Si_2W_{18}Nb_6O_{77}^{8-}$ exhibiting a parent ion due to $H_7Si_2W_{18}Nb_6O_{77}^-$ (m/z 5162) has been obtained[13a] and will be published else-

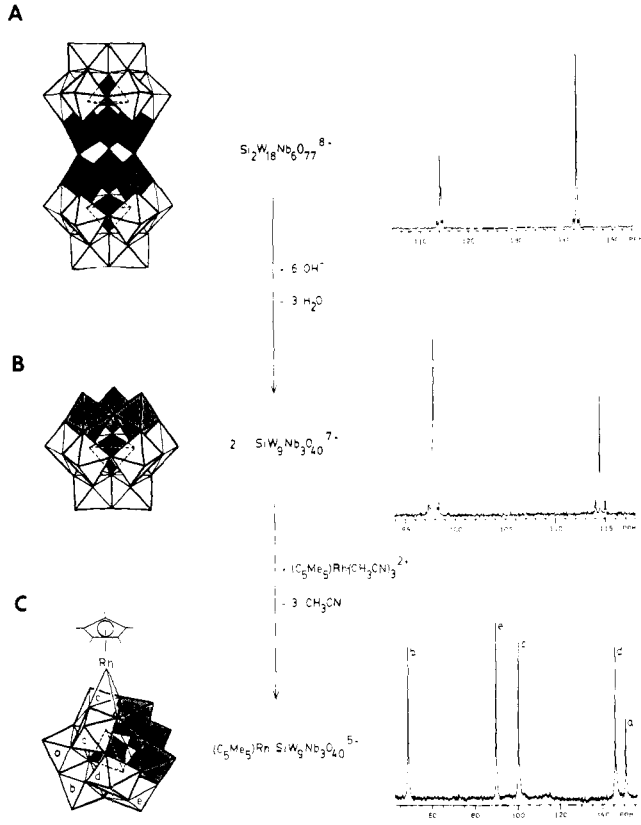

Figure 1. (A) Idealized polyhedra representation of $Si_2W_{18}Nb_6O_{77}^{8-}$. The heterogroup, SiO_4, is represented by the internal black tetrahedra, white octahedra are WO_6 groups, and the six central dark octahedra are NbO_6 units. The β,β isomer[3c] shown is expected on the basis of the β-$SiW_9O_{34}^{10-}$ precursor and is supported by the A-β structure of $[(C_5Me_5)Rh \cdot SiW_9Nb_3O_{40}]^{5-}$ established from[3e] its $^2J_{W\text{-}O\text{-}W}$ coupling constants. The right-hand part of Figure 1A shows the 15-MHz ^{183}W NMR of 0.14 M $(Bu_4N)_6H_2Si_2W_{18}Nb_6O_{77}$ in 1:1 DMF/CD_3CN. Spectra were recorded on a Nicolet NT-360 spectrometer at 21 °C using 10-mm sample tubes, $\pi/2$ pulse of 70 μs, repetition rate = acquisition time (ca. 0.8 s), and 60 000–70 000 scans. Chemical shifts are negative toward higher field and are referenced to external Na_2WO_4 saturated in D_2O at 21 °C. (B) Cleavage of the three key Nb–O–Nb linkages by base, $Si_2W_{18}Nb_6O_{77}^{8-} + 6OH^-$ to give $2SiW_9Nb_3O_{40}^{7-} + 3H_2O$. The right-hand part of Figure 1B shows ^{183}W NMR of the reaction mixture of $(Bu_4N)_6H_2Si_2W_{18}Nb_6O_{77}$ + 8Bu_4NOH (40% Bu_4NOH in H_2O) + 2 mL of CD_3CN. NMR conditions are the same as in part A. If the product in H_2O/CD_3CN is stripped to dryness and redissolved in CD_3CN the observed two-line spectrum is shifted downfield to −97.9 ± 0.1 (6 W) and −114.5 ± 0.1 ppm (3 W). (C) Structure of $[(C_5Me_5)Rh \cdot SiW_9Nb_3O_{40}]^{5-}$ showing inner-sphere, covalent attachment of the $(C_5Me_5)Rh^{2+}$ cation to three bridging oxygens of a B-type triad of edge-sharing NbW_2 octahedra. The right-hand part of Figure 1C shows the ^{183}W NMR of 0.5 M $(Bu_4N)_5[(C_5Me_5)Rh \cdot SiW_9Nb_3O_{40}]$ in CD_3CN at 60 °C with 100 000 transients and other NMR conditions as in part A. Assignments, a–e, are based on the relative intensities and especially upon the $^2J_{W\text{-}O\text{-}W}$ coupling constants.[14]

(3) (a) We were led to the use of A-type $SiW_9O_{34}^{10-}$ and higher valent M^{5+} and M^{4+} metals following our studies demonstrating that B-type $PW_9O_{34}^{9-}$ and B-type $P_2W_{15}O_{56}^{12-}$ with low-valent metals like M = Co^{2+} and Zn^{2+} lead to the disubstituted dimers[3b,c] $[PW_9M_2(H_2O)O_{34}]_2^{10-}$ and $[P_2W_{15}M_2(H_2O)O_{56}]_2^{16-}$. (b) Finke, R. G.; Droege, M.; Hutchinson, J. R.; Gansow, O. *J. Am. Chem. Soc.* **1981**, *103*, 1587. (c) Finke, R. G.; Droege, M. W. *Inorg. Chem.* **1983**, *22*, 1006. (d) Finke, R. G.; Rapko, B., manuscript in preparation. (e) Finke, R. G.; Droege, M. W., manuscripts in preparation.

(4) (a) Nonorganic solvent soluble forms of[4b] $SiW_9V_3O_{40}^{7-}$ and[4c] $P_2W_{15}V_3O_{62}^{9-}$ have been described but without synthetic details in the case of the former.[4b] (b) Mossoba, M. M.; O'Connor, C. J.; Pope, M. T.; Sinn, E.; Hervé, G.; Tézé, A. *J. Am. Chem. Soc.* **1980**, *102*, 6864. (c) Harmalker, S. P.; Leparulo, M. A.; Pope, M. T. *J. Am. Chem. Soc.* **1983**, *105*, 4286.

(5) (a) Flynn, C. M., Jr.; Stucky, G. D. *Inorg. Chem.* **1969**, *8*, 178. (b) Flynn, C. M., Jr.; Stucky, G. D. *Inorg. Chem.* **1969**, *8*, 335.

(6) (a) Besecker, C. J.; Klemperer, W. G.; Day, V. W. *J. Am. Chem. Soc.* **1982**, *104*, 6158. (b) Besecker, C. J.; Klemperer, W. G. *J. Am. Chem. Soc.* **1980**, *102*, 7598. (c) Day, V. W.; Fredrick, M. F.; Thompson, M. R.; Klemperer, W. G.; Liu, R. S.; Shum, W. *J. Am. Chem. Soc.* **1981**, *103*, 3597. (d) Besecker, C. J.; Day, V. W.; Klemperer, W. G.; Thompson, M. R.; *J. Am. Chem. Soc.* **1984**, *106*, 4125. We thank Professor Klemperer for providing us with a preprint of this manuscript and for helpful discussions.

(7) Domaille, P. J.; Knoth, W. H. *Inorg. Chem.* **1983**, *22*, 818.

(8) Fairbrother, F. "The Chemistry of Niobium and Tantalum"; Elsevier: Amsterdam, 1967.

(9) Filowitz, M.; Ho, R. K. C.; Klemperer, W. G.; Shum, W. *Inorg. Chem.* **1979**, *18*, 93.

(10) (a) Hervé, G.; Tézé, A. *Inorg. Chem.* **1977**, *16*, 2115. (b) Robert, F.; Tézé, A. *Acta Crystallogr., Sect. B* **1981**, *B37*, 318.

(11) (a) Dabbabi, M.; Boyer, M. *J. Inorg. Nucl. Chem.* **1976**, *38*, 1011. (b) The expected products of $Nb_6O_{19}^{8-}$ with H_2O_2 are the orthoperoxyniobate,[11c,d] $Nb(\mu_2O_2)_4^{3-}$, and then, under H^+, the monoperoxy complex,[11d] $Nb(O)_2(\mu_2O_2)^-$. (c) Reference 8, p 67. (d) Connor, J. A.; Ebsworth, E. A. V. *Adv. Inorg. Chem. Radiochem.* **1964**, *6*, 279.

(12) (a) Ilmaier, B. *Montsh. Chem.* **1975**, *106*, 657. (b) Buchler, J. W.; Rohbock, K. *Inorg. Nucl. Chem. Lett.* **1972**, *8*, 1073.

where.[13b] The ^{183}W NMR of $(Bu_4N)_6H_2Si_2W_{18}Nb_6O_{77}$ in 1:1 DMF/CD_3CN shows a two-line spectrum (Figure 1A) with peaks at -114.3 ± 0.1 and -142.6 ± 0.1 ppm of relative intensities 1:2, respectively, consistent with the D_{3h} symmetry dimer shown in Figure 1A. The observation of D_{3h} symmetry on the ^{183}W NMR timescale requires either the H^+ exist as H_3O^+ counterions or that protonated $H_2Si_2W_{18}Nb_6O_{77}^{6-}$ exhibit rapid proton fluxionality. A ^{183}W NMR titration in CH_3CN as a function of equivalents of 40% $Bu_4N^+OH^-/H_2O$ shows no change until >2.0 equiv of $Bu_4N^+OH^-$ are added, consistent with the presence of two H_3O^+. The $^2J_{W-O-W}$ coupling of 18.3 ± 1.2 Hz in Figure 1A requires[14] preservation of the A-type $SiW_9O_{34}^{10-}$ structure[10a] present in the A-$Na_9HSiW_9O_{34}\cdot 23H_2O$ starting material.[10b]

The presence of the Nb–O–Nb bonds linking the two $SiW_9Nb_3O_{37}^{-1}$ units suggests that reagents known to cleave the Nb–O–Nb bonds in polymeric hydrous niobium oxide,[8] $[Nb_2O_5\cdot XH_2O]_y$, might also cleave the $Si_2W_{18}Nb_6O_{77}^{8-}$ dimer. As anticipated, the known reactions of $[Nb_2O_5\cdot XH_2O]_y$ with H_2O_2, $HOCH_2CH_2NH_2$, and OH^- are also observed for $Si_2W_{18}Nb_6O_{77}^{8-}$ as easily monitored by the loss of the 690-cm^{-1} IR band and by ^{183}W NMR.

In the case of $8Bu_4N^+OH^- + (Bu_4N)_6(H_3O)_2Si_2W_{18}Nb_6O_{77} \rightarrow 7H_2O + 2(Bu_4N)_7SiW_9Nb_3O_{40}$, this stoichiometry and the presence of two H_3O^+ were quantitatively confirmed by an IR titration in CH_3CN vs equivalents of added 40% $Bu_4N^+OH^-/H_2O$. No change in absorbance of the 690-cm^{-1} band is observed until 2.0 equiv of $Bu_4N^+OH^-$, at which a sharp breakpoint and a linear decrease to zero absorbance at 8.0 equiv are observed. The monomer formed, $SiW_9Nb_3O_{40}^{7-}$ by the reaction stoichiometry, was further characterized by solution molecular weight measurements in CH_3CN (calcd for $SiW_9Nb_3O_{40}^{7-}$, 2601; calcd for $(Bu_4N)_2SiW_9Nb_3O_{40}^{5-}$, 3085; found, 3179; available as supplementary materials) by a FABMS in 5:1 dithiothreitol/dithioerythritol showing a parent ion for the $H_6SiW_9Nb_3O_{40}^-$ (m/z 2608) and by the ^{183}W NMR provided in Figure 1B, exhibiting peaks at -112.0 ± 0.1 ppm (6 W, $^2J_{W-O-W} = 15.3 \pm 1.2$ Hz) and -122.1 ± 0.1 ppm (3 W, $^2J_{W-O-W} = 15.3 \pm 1.2$ Hz). The larger ^{183}W resonance is now downfield of the smaller one as is observed for[3d] $SiW_9V_3O_{40}^{7-}$. Upon reacidification, the dimer is completely reformed (^{183}W NMR, IR). It is noteworthy that cleavage can be accomplished without detectable $SiW_9Nb_3O_{40}^{7-}$ decomposition by using a base as strong as OH^-. Traditional heteropolytungstates such as $SiW_{12}O_{40}^{4-}$ are rapidly decomposed by OH^- to SiO_3^{2-} and WO_4^{3-}, although counterions like Bu_4N^+ and organic solvents like CH_3CN dramatically inhibit this process.[15]

The cleavage reactions suggest that $Si_2W_{18}Nb_6O_{77}^{8-}$ behaves, in effect, as a solubilized piece of niobium oxide $[Nb_2O_5]_3$, sandwiched between two "$SiW_9O_{31}^{4-n}$ heteropolyanion fragments.[16] This analogy suggests an extensive, undeveloped chemistry of V-, Nb-, Ti-, Zr-, Cr-, and other M-substituted polyoxoanions as homogeneous analogues of V_2O_5, Nb_2O_5, TiO_2, ZrO_2, ZnO, Fe_2O_3, Cr_2O_3, and other M_xO_y solid oxides. A larger, previously unappreciated class[17] of dimeric and oligomeric polyoxoanions is also indicated.

The first structurally characterized organometallic complex supported on a substituted Keggin anion was prepared by the addition of 0.75 mmol of orange $[(C_5Me_5)Rh(CH_3CN)_3](BF_4)_2$[18] to 0.75 mmol of colorless solid[19] $(Bu_4N)_7SiW_9Nb_3O_{40}$ dissolved in 60 mL of CH_3CN. The initially formed yellow solid, probably due to $(C_5Me_5)Rh(CH_3CN)_3^{2+}$ acting as a simple outer-sphere counterion to $SiW_9Nb_3O_{40}^{7-}$, quickly redissolved to yield an orange-red solution, which was refluxed until the ^{183}W NMR simplified to a clean, five-line pattern (1 h). Solvent removal under vacuum gave a thick red oil, which became a red-orange solid under high vacuum for 5 h.

The product's homogeneity, composition, and structure, and the inner-sphere, covalent attachment of $(C_5Me_5)Rh^{2+}$ are established by FABMS, IR, ^1H NMR, ^{183}W NMR, and ion-exchange studies. A $\delta(CD_3CN)$ 1.83 singlet for the C_5Me_5 ligand in the 360-MHz ^1H NMR indicates a single product as does the clean, high S/N ^{183}W NMR (vide infra). A positive ion FABMS in 5:1 dithiothreitol/dithioerythritol shows a $\{(Bu_4N)_5H[(C_5Me_5)Rh\cdot SiW_9Nb_3O_{40}]\}^+$ molecular ion at m/z 4053. ^1H NMR and IR (KBr) confirm that the CH_3CN previously coordinated to rhodium in $(C_5Me_5)Rh(CH_3CN)_3^{2+}$ is now absent, implying inner-sphere attachment of $(C_5Me_5)Rh^{2+}$ to $SiW_9Nb_3O_{40}^{7-}$. Furthermore, ion-exchange studies demonstrate that the highly colored $[(C_5Me_5)Rh\cdot SiW_9Nb_3O_{40}]^{5-}$ passes unaltered (^1H, ^{183}W NMR) through an Amberlyst 15 cation exchange resin (Bu_4N^+ form in CH_3CN), while a control shows orange $(C_5Me_5)Rh(CH_3CN)_3^{2+}$ is retained at the top of the column. Similarly, all the color of $(Bu_4N)_5[(C_5Me_5)Rh\cdot SiW_9Nb_3O_{40}]$ is retained by an Amberlyst A-27 anion-exchange column (Cl^- form in CH_3CN). ^{183}W NMR and IR studies establish that $(C_5Me_5)Rh^{2+}$ is attached to a B-type[3b,c] triad of edge-sharing Nb_2W octahedra in $SiW_9Nb_3O_{40}^{7-}$ (Figure 1C). The ^{183}W NMR (CD_3CN) (Figure 1C), shows a five-line pattern with signals of 2:2:2:2:1 relative intensity at δ (± 0.1) ($^2J_{W-O-W} \pm 0.6$ Hz, assignment) of -49.2 (16.2 Hz, b), -90.4 (≤ 10 Hz (not obsd), e), 101.0 (14.0 and 29.3 Hz, c), -146.3 (15.9 and 30.2 Hz, d), and -151.1 (12.8 Hz, a), establishing the C_s symmetry of the complex. Solution (CH_3CN) IR shows that the broad, 800-cm^{-1} band in $(Bu_4N)_7SiW_9Nb_3O_{40}$ assigned[20] to an M–O–M stretch of *edge-sharing* octahedra is split in $(Bu_4N)_5[(C_5Me_5)Rh\cdot SiW_9Nb_3O_{40}]$ by 30 cm^{-1} into distinct components at 820 and 790 cm^{-1}. The data are consistent with and fully supportive of covalent attachment of $(C_5Me_5)Rh^{2+}$ to the NbW_2 site as shown in Figure 1C. This site preference for the NbW_2 triad, B-type site of edge-sharing octahedra over the Nb_3 triad, A-type site of corner-sharing octahedra most likely reflects the smaller steric interactions[6d] between the terminal M=O (M = Nb, W) and the C_5Me_5 group in the B-type site.

In future publications[3e] we will present the additional structural insights provided by the $^2J_{W-O-W}$ coupling constants for $[(C_5Me_5)Rh\cdot SiW_9Nb_3O_{40}]^{5-}$, the characterization of the products of H_2O_2 and $HOCH_2CH_2NH_2$ cleavage of $Si_2W_{18}Nb_6O_{77}^{8-}$, the reactions of the H_2O_2 cleavage product, the synthesis, structure, and 2-D NMR of crystalline $(Bu_4N)_4[CpTi\cdot SiW_9V_3O_{40}]$,[3d] and other results with members of the $SiW_9M_3O_{40}^{x-}$ and $P_2W_{15}M_3O_{62}^{y-}$ series.

Acknowledgment. Support from NSF Grant CHE-8313459 and from Dreyfus Teacher-Scholar (1982–1987) and Alfred P. Sloan (1982–1984) Fellowships to R.G.F. are gratefully acknowledged. We also acknowledge the fine technical skill of

(13) (a) The first mass spectra of polyoxoanions, obtained by FABMS, is described in: Finke, R. G.; Droege, M. W.; Cook, J. C.; Suslick, K. S. *J. Am. Chem. Soc.* **1984**, *106*, 5750. (b) Suslick, K. S.; Cook, J. C.; Droege, M. W.; Finke, R. G. *J. Chem. Soc., Chem. Commun.*, submitted for publication.

(14) (a) Lefebvre, J.; Chauveau, F.; Doppelt, P.; Brevard, C. *J. Am. Chem. Soc.* **1981**, *103*, 4589. (b) Knoth, W. H.; Domaille, P. J.; Roe, D. C. *Inorg. Chem.* **1983**, *22*, 198. (c) Reference 7, p 820. (d) Brevard, C.; Schimpf, R.; Tourne, G.; Tourne, C. M. *J. Am. Chem. Soc.* **1983**, *105*, 7059.

(15) (a) Kepert, D. L.; Kyle, J. H. *J. Chem. Soc., Dalton Trans.* **1978**, 137. (b) Kepert, D. L.; Kyle, J. H. *J. Chem. Soc., Dalton Trans.* **1978**, 1781.

(16) (a) The metal oxide minisurface of a trisubstituted heteropolytungstate such as $SiW_9Nb_3O_{40}^{7-}$ cannot, of course, mimic the complicated 3-dimensional structure and many polymorphs of Nb_2O_5.[16b,c] The structural analogy is good, however, for binary oxides such as ZnO.[3b] (b) Wells, A. F. "Structural Inorganic Chemistry", 4th ed.; Clarendon Press: Oxford, England, 1975. (c) For the structure of H–Nb_2O_5, see: Gatehouse, B. M.; Wadsley, A. D. *Acta Crystallogr.* **1964**, *17*, 1545.

(17) (a) Zonnevijlle, F.; Tournē, C. M.; Tournē, G. F. *Inorg. Chem.* **1982**, *21*, 2751. (b) The X-ray diffraction structure of polymeric $(AsCoW_{11}O_{39})^{5n-}$ linked by Co–O–W bridges has been described: Weakley, T. J. R. *Proc. Jt. NSF-CNRS Polyoxoanion Workshop* **1983**, 30.

(18) White, C.; Thompson, S. J.; Maitlis, P. M. *J. Chem. Soc., Dalton Trans.* **1977**, 1654.

(19) Solid $(Bu_4N)_7SiW_9Nb_3O_{40}$ was prepared from 5.0 g of $(Bu_4N)_6H_2Si_2W_{18}Nb_6O_{77}$ (0.75 mmol) and 3.71 mL of 1.63 M $Bu_4N^+OH^-/H_2O$ (6.05 mmol) in 50 mL of CH_3CN followed by removal of the CH_3CN under vacuum and, if necessary, solidification of the thick oil by drying at 80 °C under vacuum for 2–3 h. Recrystallization of salts with $>4Bu_4N^+$ such as $(Bu_4N)_7SiW_9Nb_3O_{40}$ or $(Bu_4N)_5[(C_5Me_5)Rh\cdot SiW_9Nb_3O_{40}]$ has not, to date, been successful although their high solubility allowing good S/N ^{183}W NMR has proven to be a major advantage.

(20) Thouvenot, R.; Fournier, M.; Franck, R.; Rocchiccioli-Deltcheff, C. *Inorg. Chem.* **1984**, *23*, 598.

George Gessert in providing illustrations of polyoxoanions appearing here and in our previous publications.[3]

Supplementary Material Available: Detailed synthetic procedures for the synthesis of $(Bu_4N)_6H_2Si_2W_{18}Nb_6O_{77}$ and $(Bu_4N)_7HSi_2W_{18}Nb_6O_{77}$; IR data and the ultracentrifugation solution molecular weight measurements on $Si_2W_{18}Nb_6O_{77}^{8-}$ and $SiW_9Nb_3O_{40}^{7-}$ (7 pages). Ordering information is given on any current masthead page.

Alternative Precursors to 1,4-Acyl Alkyl Biradicals: Cyclic *N*-Acyl-1,1-diazenes

R. D. Miller,* P. Gölitz, J. Janssen, and J. Lemmens

IBM Research Laboratory, San Jose, California 95193

Received February 17, 1984

The photochemistry of cyclobutanone derivatives is unique relative to other cycloalkanones both with regard to the nature and stereoselectivity of the photoprocesses.[1] The regioselectivity has been rationalized in terms of initial α cleavage to form the most stable acyl alkyl biradical. In order to reconcile the high stereoselectivities for product formation and the lack of isomerization in the starting materials, it is necessary to postulate that the subsequent reactions of the proposed biradical are rapid with respect to bond rotation. In addition, theoretical studies have suggested that the acyl alkyl biradical is not necessarily even an intermediate[2] in the unusual photochemistry ring expansion to form oxacarbenes in protic solvents.

While there has been considerable experimental and theoretical efforts directed toward understanding the photochemistry of cyclobutanone derivatives, many questions still remain regarding the proposed intermediates.[1] What is clearly needed is an alternative source of 1,4-acyl alkyl biradicals in order to compare the chemistry with that observed from photolysis. Accordingly, we describe here the in situ generation and decomposition of the cyclic N-acyl-1,1-diazenes[3] **2a–d** as alternative sources of 1,4-acyl alkyl biradicals and discuss the similarity and differences relative to the photochemistry of the corresponding substituted cyclobutanones **4a–d**.

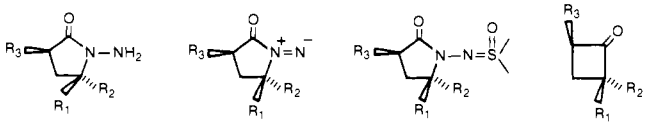

2a-d 3a-d 4a-d

1a $R_1=R_2=Ph$, $R_3=H$
1b $R_1=Me$, $R_2=Ph$, $R_3=H$
1c $R_1=Me$, $R_2=Ph$, $R_3=Me$
1d $R_1=Ph$, $R_2=Me$, $R_3=Me$

Since 1,1-diazene–dimethyl sulfoxide adducts have been described as useful in situ thermal and photochemical sources of the corresponding 1,1-diazenes,[4] we prepared the sulfoximines **3a,b** by the oxidation of **1a** and **1b**[5] with lead tetraacetate in the presence of Me_2SO. The thermal decomposition of **3a,b** followed first-order kinetics over the measurement interval (70–110 °C). The mass balance of volatile products was >95% and the results are shown in Table I[6] in comparison with those from the photochemical decomposition of the corresponding cyclobutanones **4a,b**.[7] It is obvious that although the cyclobutanones **4a** and **4b** are the major products from the decomposition of **3a** and **3b**, the relative proportion of olefin from β-elimination and the cyclopropane from decarbonylation both increase with temperature. No significant external heavy atom effect was observed when **3a** was decomposed in dibromomethane (entry 3). In methanol the cyclic acetals (see Table I) were major products. The use of methanol-d_1 in the decomposition of **3a** resulted in the formation of cyclic acetal which was >90% (^{1}H NMR and mass spectroscopic analysis) deuterated at the methine site of the acetal carbon atom. This result strongly suggests that the corresponding cyclic oxacarbene is an intermediate in the thermal process and demonstrates unambiguously that these intermediates can result from the cyclization of 1,4-acyl alkyl biradicals. Another remarkable feature is the observed *increase* in the relative yield of the cyclic acetals (Table I, entries 5 and 11) at the lower temperatures. In this regard, Agosta and co-workers[8] have previously reported cyclobutanones as major products from cyclic oxacarbenes generated pyrolytically, thus establishing a possible alternative thermal reaction pathway for

Table I[a]

Cmpd	Entry	Reaction Conditions					
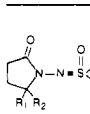 3a $R_1=R_2=Ph$	1		100°	11.6	8.2	80.2	–
				(58.5)[b]	(41.4)[b]	–	–
	2		25°[b]	8.8	5.1	88.0	–
				(54.1)	(42.8)	–	–
	3	CH_2Br_2	100°	13.2	10.2	76.4	–
	4	MeOH	100°	8.3	6.9	78.3	6.5
				(38.2)	(31.7)	–	(30.0)
	5		25°[b]	2.5	1.6	–	10.9
				(16.7)	(10.7)	–	(72.6)
 4a	6	hv,  (0.12)[c,d]	25°	8.1	19	–	–
	7	hv, MeOH (0.13)[c,d]	25°	58	14	–	28
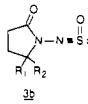 3b $R_1=Ph$, $R_2=Me$	8		100°	7.4	11.3	78.5	–
				(39.5)	(60.4)	–	
	9		25°[b]	5.0	8.2	86.7	–
				(37.8)	(62.1)	–	
	10	MeOH	100°	3.6	6.9	69.0	20.4
				(11.7)	(22.3)	–	(66.0)
	11		25°[b]	1.3	3.8	66.5	28.3
				(3.8)	(11.3)	–	(84.2)
 4b	12	hv, 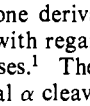 (0.12)[c,d]	25°	76	24	–	–
	13	hv, MeOH (0.11)[c,d]	25°	37	12	–	51

[a] Thermolysis products from **3a** and **3b**. Tubes were freeze–thaw degassed and sealed. The mass balance of volatile products was >95%. (a) Relative product yields excluding ring closure; (b) product yields extrapolated to 25 °C from measurements made between 70 and 110 °C; (c) solutions for irradiation (0.05 M) were degassed and sealed in Pyrex tubes: (d) quantum yields were determined at 313 nm by using a calibrated thermopile from Eppley Laboratory, Inc., to determine the light intensity; yields were determined by GLPC analysis at low conversions (<20%).

(1) For an excellent review of the photochemistry of cyclobutanone derivatives, see: Morton, D. R.; Turro, N. J. *Adv. Photochem.* **1974**, *9*, 197 and references cited therein.

(2) (a) Quinkert, G.; Jacobs, P.; Stohrer, W.-D. *Agnew. Chem., Int. Ed. Engl.* **1974**, *13*, 197. (b) Quinkert, G.; Kaiser, K. H.; Stohrer, W.-D. *Angew. Chem., Int. Ed. Engl.* **1974**, *13*, 98. (c) Stohrer, W.-D.; Weich, G.; Quinkert, G. *Angew. Chem., Int. Ed. Engl.* **1974**, *13*, 199. (d) Stohrer, W.-D.; Weich, G.; Quinkert, G. *Angew. Chem., Int. Ed. Engl.* **1974**, *13*, 200.

(3) Recently, Dervan and co-workers have described the spectral characterization of some persistent cycloalkyl 1,1-diazenes and studied their use as radical precursors: (a) Hinsberg, W.-D. III; Schultz, P. G.; Dervan, P. B. *J. Am. Chem. Soc.* **1982**, *104*, 766. (b) Schultz, P. G.; Dervan, P. B. *J. Am. Chem. Soc.* **1982**, *104*, 6660. (c) McIntyre, D. K.; Dervan, P. B. *J. Am. Chem. Soc.* **1982**, *104*, 6466. (d) Dervan, P. B.; Squillacote, M. E.; Lahti, P. M.; Sylvester, A. P.; Roberts, J. D. *J. Am. Chem. Soc.* **1981**, *103*, 1120.

(4) (a) Andersen, D. J.; Gilchrist, T. L.; Horwell, D. C.; Rees, C. W. *J. Chem. Soc., Chem. Commun.* **1969**, 146. (b) Gilchrist, T. L.; Rees, C. W.; Stanton, E. *J. Chem. Soc.* C **1971**, 988. Andersen, D. J.; Horwell, D. C.; Stanton, E. *J. Chem. Soc., Perkin Trans. 1* **1972**, 1317. (d) Kim, M.; White, J. D. *J. Am. Chem. Soc.* **1974**, *98*, 451.

(5) Miller, R. V.; Gölitz, P.; Janssen, J.; Lemmens, J. *J. Am. Chem. Soc.* **1984**, *106*, 1508.

(6) The structure of all new compounds is supported by analytical and spectral data.

(7) Trost, B. M.; Bogdanowicz, M. J. *J. Am. Chem. Soc.* **1973**, *95*, 5321.

(8) (a) Agosta, W. C.; Foster, A. M. *J. Chem. Soc., Chem. Commun.* **1971**, 433. (b) Foster, A. M.; Agosta, W. C. *J. Am. Chem. Soc.* **1972**, *94*, 5777. (c) Foster, A. M.; Agosta, W. C. *J. Am. Chem. Soc.* **1973**, *95*, 608.

0002-7863/84/1506-7277$01.50/0